Optics Letters

Spectral compression using time-varying cavities

KARTHIK V. MYILSWAMY[1] AND ANDREW M. WEINER[1,2,3,*]

[1]School of Electrical and Computer Engineering, Purdue University, West Lafayette, Indiana 47906, USA
[2]Purdue Quantum Center, Purdue University, West Lafayette, Indiana 47906, USA
[3]Birck Nanotechnology Center, Purdue University, West Lafayette, Indiana 47906, USA
*Corresponding author: amw@purdue.edu

Received 7 August 2020; revised 18 September 2020; accepted 21 September 2020; posted 21 September 2020 (Doc. ID 404891); published 7 October 2020

Spectral compression will be needed for efficient interfacing of broadband photons with narrowband quantum memories for applications in quantum information and networking. In this Letter, we propose spectral compression via a time-varying, linear optical cavity. Unlike other recent works on time-varying cavities based on modulation of the intracavity phase, our spectral compression concept is based on rapid switching of coupling into the cavity. We analyze spectral compression performance metrics as a function of mirror reflectivity, cavity loss, and switching speed and discuss potential implementation in integrated photonics.

https://doi.org/10.1364/OL.404891

Linear, time-invariant optical cavities are used widely as spectral filters. However, several new phenomena arise when linear cavities are actively modulated. Dynamical tuning of the refractive index has been exploited to experimentally demonstrate adiabatic wavelength conversion in optical cavities [1,2], on-chip nonreciprocal transmission of light [3], frequency comb generation in electro-optic cavities [4–6], and optical storage, retrieval, and manipulation in active photonic molecule structures [7,8]. Numerical studies involving coupled cavities, subjected to dynamic refractive index tuning, predict more novel phenomena including stopping, coherent storage, and time reversal of light [9]. Dynamically coupled nonlinear cavities have also been proposed to achieve high fidelity deterministic quantum gates for photonic qubits [10]. It is important to note that the dynamical tuning of the cavity for such applications should be achieved in a time scale much shorter than that of the photon lifetime.

In this Letter, we propose and analyze the use of time-varying cavities for spectral compression. Unlike the time-varying cavities cited above, which are all based on modulation of the intracavity phase, our spectral compression concept is based on rapid switching of coupling into the cavity. In view of strong interest in quantum information and quantum networking [11], spectral compression is needed to efficiently interface broadband photons, such as those from parametric down-conversion sources, with narrowband nodes, such as quantum dots, color centers, and atomic systems. Spectral compression has also been employed in classical applications such as absorption spectroscopy [12] and nonlinear (especially Raman) microscopy [13]. Prior approaches to spectral compression have for the most part relied on nonlinear optical schemes, including self-phase modulation of down-chirped pulses in conventional optical fibers [13], soliton propagation in dispersion-increasing fibers [12,14], sum frequency mixing of broadband pulses with opposite chirps [15], and second-harmonic generation [16,17] and sum frequency mixing [18] in thick nonlinear crystals with phase matching characteristics dominated by group velocity mismatch. Spectral compression has also been reported using dispersive propagation followed by electro-optic phase modulation, i.e., time lens operation [19–21]. Reference [21], in which the bandwidth of single photons was compressed from 150 GHz to 1.46 GHz, offers one of the most extreme experimental examples. In this Letter, we propose a new route to spectral compression, in which a relatively broadband pulse is captured into a time-varying cavity via electro-optic switching of the input coupling. By using low loss, high Q cavities, it should be possible to realize spectral compression, potentially to well below 1 GHz, limited only by the cavity linewidth. This concept is inspired by previous work on the virtually imaged phase array (VIPA) [22–24], a cavity that violates translational space invariance resulting in compression of the spatial frequency spectrum. In this work, we violate the time invariance of the cavity by switching the input reflectivity, which results in spectral compression following space–time duality.

It is commonly known in the context of mode-locked lasers and frequency combs that when multiple evenly spaced, phase-locked frequency modes are present, the resultant temporal pulse width decreases in inverse proportion to the number of frequency modes [25]. As time and frequency obey the duality property of Fourier transform, we expect that forming multiple, phase-locked temporal copies of the same pulse should result in a decrease in the spectral width. One of the most straightforward ways to obtain multiple temporal copies is to use an optical cavity. Without loss of generality, for now we consider a Fabry–Perot (FP) cavity, although our concept is applicable to any generic cavity structure. As is well known, a pulse incident on a FP cavity suffers strong reflection of frequencies that are significantly detuned from the cavity resonance. Hence, even if the cavity transmission is unity on resonance, an isolated input pulse suffers strong insertion loss. We propose to avoid these losses by rapidly switching the reflectivity of the input mirror from zero to unity just after the pulse enters the cavity (Fig. 1). If there is no loss, the entire power has to eventually then exit through the

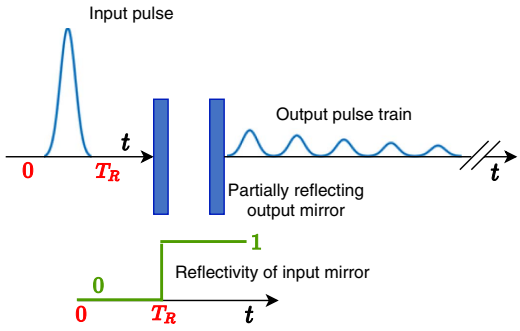

Fig. 1. Time-varying cavity with input mirror reflectivity rapidly switched from zero to unity after the pulse enters the cavity. The output mirror is partially reflecting (power reflectivity of 0.8 is chosen for this illustration). In contrast to FP cavity, no reflection occurs onto the input side. All the energy exits through the output mirror creating an output pulse train with decreasing amplitude resulting in spectral compression.

partially reflecting output mirror. The output contains multiple copies of the input pulse with decreasing amplitude. They have fixed relative delay (corresponding to cavity roundtrip time) and are phase locked to each other. This effectively leads to spectral compression (spectral narrowing along with increased peak power spectral density), as energy conservation is ensured.

Consider a FP cavity with an input mirror (field reflection and transmission coefficients given by r_1 and t_1, respectively) and an output mirror (field reflection and transmission coefficients given by r_2 and t_2, respectively) of roundtrip time T_R. The relationship between the input (E_{in}) and output (E_{out}) fields of the FP cavity in time and frequency domains are given by Eq. (1):

$$E_{\text{out}}(t) = \sum_{m=0}^{\infty} t_1 t_2 (r_1 r_2)^m E_{\text{in}}\left[t - \left(m T_R + \frac{T_R}{2}\right)\right],$$

$$E_{\text{out}}(\omega) = \frac{t_1 t_2 e^{-j\omega\frac{T_R}{2}}}{1 - r_1 r_2 e^{-j\omega T_R}} E_{in}(\omega). \tag{1}$$

Now let us consider a time-varying cavity (Fig. 1) whose input reflection coefficient r_1 is rapidly switched from zero to one at $t = T_R$. For pulses of width lesser than that of T_R that are input within $t = 0$ and $t = T_R$, the output of such a time-varying cavity is given by Eq. (2). Here, we have essentially switched the reflectivity after the entire pulse energy has been captured inside the cavity. It can be seen that the given relationship is similar to that of the FP cavity, except for terms r_1 and t_1 getting identically replaced by one, as a result of rapid switching:

$$E_{\text{out}}(t) = \sum_{m=0}^{\infty} t_2 (r_2)^m E_{\text{in}}\left[t - \left(m T_R + \frac{T_R}{2}\right)\right],$$

$$E_{\text{out}}(\omega) = \frac{t_2 e^{-j\omega\frac{T_R}{2}}}{1 - r_2 e^{-j\omega T_R}} E_{\text{in}}(\omega). \tag{2}$$

The ratio between the output and input power spectral densities attains the maximum at the frequency locations corresponding to the resonance modes for both the static FP cavity and time-varying cavity; the corresponding maximum values are given by Eq. (3). In the case of a passive FP cavity (no gain), the output power spectral density is less than or equal to the input at all frequencies (spectral filtering). However, interestingly in the case of the time-varying cavity, the output power spectral density exceeds that of the input at multiple frequency locations [ratio shown in inset of Fig. 2(c)]; this constitutes spectral compression:

FP cavity:

$$\text{Max}\left\{\left|\frac{E_{\text{out}}(\omega)}{E_{\text{in}}(\omega)}\right|^2\right\} = 1 - \left(\frac{|r_1| - |r_2|}{1 - |r_1||r_2|}\right)^2 \leq 1,$$

Time-varying cavity :

$$\text{Max}\left\{\left|\frac{E_{\text{out}}(\omega)}{E_{\text{in}}(\omega)}\right|^2\right\} = 1 + \left(\frac{2|r_2|}{1 - |r_2|}\right) \geq 1. \tag{3}$$

We present an example by considering a flat-topped pulse of width T_R, with sinusoidal leading and trailing edges that together account for a net 25% of the pulse width [see inset of Fig. 2(d)], at a carrier frequency coinciding with one of the resonance modes of the cavity. Here, by pulse width, we refer to the entire time window over which the intensity is nonzero. The pulse is input into the cavity between $t = 0$ and $t = T_R$. In the case of the time-varying cavity, the input mirror reflectivity is switched from zero to one at $t = T_R$. The output power spectrum for both the FP cavity ($r_1 = r_2 = 0.95$) and the time-varying cavity ($r_2 = 0.95$) are plotted in Figs. 2(a) and 2(b), respectively. This clearly illustrates the entirely different spectral filtering and spectral compressing operations performed by the FP cavity and the time-varying cavity, respectively. For a similar pulse oscillating at the same resonance frequency but with a pulse width of $0.5\,T_R$, the output of the time-varying cavity is plotted in Fig. 2(c). The presence of multiple peaks, of relatively higher power, can be explained by the fact that the input power present at different cavity resonance frequencies gets enhanced by the same factor [see inset of Fig. 2(c)]. Hence, we would like to roughly match the width of the pulse with the cavity roundtrip time T_R so that the energy is compressed mostly into a single spectral peak. Also if the carrier frequency does not coincide with the cavity resonance, the spectral compression peaks occur asymmetrically with respect to the input spectral envelope. This is illustrated in Fig. 2(d) for an input pulse of width T_R, oscillating at a carrier frequency of 0.25 FSR away from a cavity resonance. Similar results are expected for other input pulse shapes, provided that the pulse duration is appropriately matched to the cavity roundtrip time.

We define a spectral compression factor as the ratio between the full width at half maximum (FWHM) of the input and output power spectral densities. Equation (3) indicates that enhancement in peak power spectral density at the output of time-varying cavity increases if $|r_2|$ is increased. Hence, the spectral compression factor that is proportional to the enhancement in peak power also increases with $|r_2|$. This can be explained by the fact that for an increased value of $|r_2|$, the pulse executes more roundtrips within the cavity and hence generates more copies of the input pulse. However in the case of cavities with nonzero loss, this results in a trade-off between achievable spectral compression and integrated loss. In the case of nonzero loss, Eq. (2) assumes the following form, where $2\alpha L$ represents the loss per roundtrip:

$$E_{\text{out}}(\omega) = \frac{t_2 e^{-\frac{\alpha L}{2}} e^{-j\omega\frac{T_R}{2}}}{1 - r_2 e^{-\alpha L} e^{-j\omega T_R}} E_{\text{in}}(\omega). \tag{4}$$

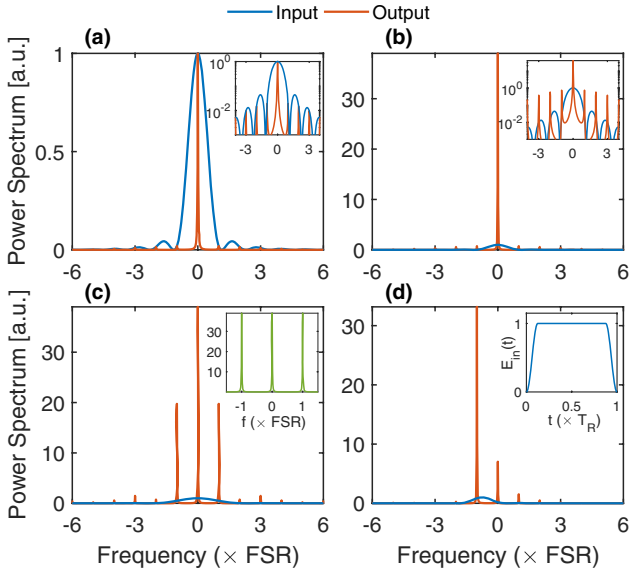

Fig. 2. Input and output power spectral densities (with respect to a specific cavity resonance frequency). Input pulse has a rectangular profile except for sinusoidal edges accounting totally for 25% of pulse width [shown in inset of (d)]. Input reflectivity of time-varying cavity is switched after the pulse enters the cavity. (a) FP cavity ($r_1 = r_2 = 0.95$) and (b) time-varying cavity ($r_2 = 0.95$) plots for a pulse of width T_R oscillating at a cavity resonance frequency. Time-varying cavity plots for pulses of (c) same carrier frequency but a width of $0.5\,T_R$ and (d) width T_R but at a carrier frequency 0.25 FSR away from a cavity resonance. Plots are normalized to corresponding maximum input power spectral density. Respective log scale plots are shown in insets of (a) and (b) to highlight the presence of multiple peaks. Inset of (c) depicts the multiplication factor between input and output power spectra of time-varying cavity.

To illustrate this trade-off, we consider a pulse [inset of Fig. 2(d)] of width T_R at a carrier frequency coinciding with one of the resonance modes, which is input into the time-varying cavity. The achievable spectral compression, integrated loss, and ratio of peak output and input power spectral densities are analytically calculated and plotted in Fig. 3 as a function of $|r_2|$, for different values of loss per roundtrip. Figure 3(a) illustrates the fact that both the spectral compression and integrated loss increase with $|r_2|$ in the case of nonzero cavity losses. However, the ratio of output and input peak power spectral densities depends on both spectral compression and integrated loss. Hence, it attains a maximum at an optimal value of $|r_2|$, depending on the cavity loss parameter as shown in Fig. 3(b); the maximum ratio decreases with the increase in cavity loss per roundtrip. This clearly shows the limitations on achievable spectral compression in a time-varying cavity with nonzero intracavity losses.

In the discussion so far, we have assumed rapid switching of the input mirror reflectivity. However, in practice, we have to consider nonzero rise time for switching the input mirror reflectivity. For any generic input mirror reflectivity function $r_1(t)[t_1(t)]$ and input pulse shape, the output and input pulses can be related using a recursive relation, which then can be expressed as a Fredholm integral that possesses a Liouville–Neumann series solution [26,27] as shown in Eq. (5):

$$E_{\text{out}}(t) = t_1\left(t - \frac{T_R}{2}\right) t_2 E_{in}\left(t - \frac{T_R}{2}\right) + r_1\left(t - \frac{T_R}{2}\right) r_2 E_{\text{out}}\,(t - T_R),$$

$$E_{\text{out}}(t) = \left\{\sum_{m=0}^{\infty} t_1\left[t - \left(m T_R + \frac{T_R}{2}\right)\right] t_2 \times E_{\text{in}}\left[t - \left(m T_R + \frac{T_R}{2}\right)\right] \prod_{n=0}^{m} b_n\right\},$$

$$b_0 = 1, \quad b_n = r_1\left[t - \left(n T_R - \frac{T_R}{2}\right)\right] r_2 \quad \forall\, n \geq 1. \tag{5}$$

In the case of nonzero rise time, a finite amount of power is reflected back onto the input side, resulting in an insertion loss. Also, the function $r_1(t)$ is going to change the temporal waveform of the input pulse affecting the spectral purity of the output. Here, we define spectral purity as the ratio between the first and second highest peaks in the output power spectral density. Ideally, we would prefer higher spectral purity and lower insertion loss. Hence, spectral purity and insertion loss can be viewed as performance metrics for spectral compression. The arrival time of the input pulse for a given pulse width and $r_1(t)$ can be optimized to realize either maximum spectral purity or minimum insertion loss. The simulated spectral purity and insertion loss, while optimizing for minimum insertion loss, are plotted as a function of rise time of $r_1(t)$ in Fig. 4, for different values of input pulse width. The input pulses are again as shown in the inset of Fig. 2(d) and oscillating at one of the resonance frequencies of the cavity. The cavity is assumed to have zero intracavity loss and an r_2 of 0.95. $r_1(t)$ is assumed to be a raised cosine function, increasing from zero to one for the given rise

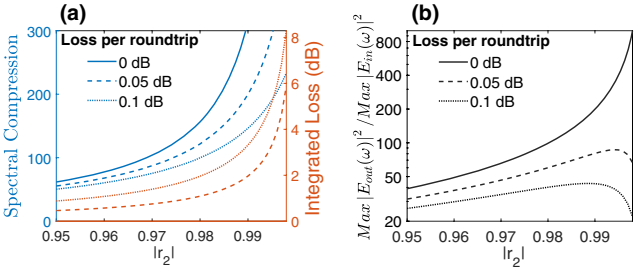

Fig. 3. (a) Spectral compression (blue) and integrated loss (red) and (b) ratio of peak output and input power spectral densities (black) as a function of $|r_2|$ for different values of loss per roundtrip: 0 dB (solid), 0.05 dB (dashed), and 0.1 dB (dotted) considering a pulse of width T_R and profile shown in inset of Fig. 2(d), which is input into the time-varying cavity.

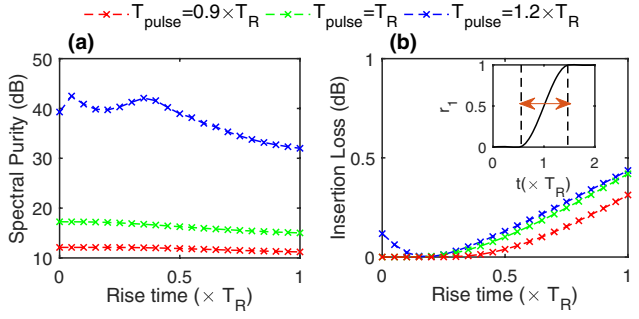

Fig. 4. Simulated (a) spectral purity and (b) insertion loss while optimizing for minimum insertion loss as a function of rise time of $r_1(t)$. $r_1(t)$ is assumed to have raised cosine form as shown in inset of (b), where the red arrow indicates the rise time. Trends are shown for input pulses [profile as shown in inset of Fig. 2(d)] of three different pulse widths.

time, as shown in the inset of Fig. 4(b). The spectral purity can be observed to have an overall decreasing trend with the increase in rise time. The highest spectral purity is associated with the case $T_{\text{pulse}} = 1.2 \times T_R$, which can be explained by the relatively lower input power spectral density at adjacent cavity resonance frequencies. The insertion loss can be seen to monotonically increase from zero with the rise time of $r_1(t)$ when $T_{\text{pulse}} \leq T_R$ and is within 0.5 dB for all values of considered rise time and pulse widths. For the case $T_{\text{pulse}} = 1.2 \times T_R$, the insertion loss is non-zero for all values of rise time, and the minimum is around 0.002 dB. This discussion illustrates the effect of cavity losses and reflectivity switching rise time on spectral compression performance.

Practically, it will be desirable to demonstrate the spectral compression in an integrated photonics platform. One of the primary requirements to realize spectral compression is the rapid switching of the input mirror reflectivity. With recent advances in on-chip modulators, especially in thin film lithium niobate (TFLN), it is possible to envision the practical demonstration of this concept. Both low-loss (∼2.7 dB/m) high Q cavities ($\sim 10^7$) and high modulation rates (∼100 GHz) have been reported in the TFLN platform [28,29]. Even though our prior discussion involved FP cavities, it can be extended to microring resonators. We propose a ring resonator cavity that is configured with a rapidly switchable variable coupler, formed from a Mach–Zehnder interferometer (MZM), as a possible device geometry to realize this concept. This allows the input pulse to be coupled with high efficiency into the cavity (MZM in cross state), after which the light is trapped (MZM switched to allow only a few percent output coupling). The losses reported in TFLN platforms are around ∼2.7 dB/m in straight waveguide sections [28], ∼0.1 dB for a phase shifter of 0.5 cm with a V_π value of 4.4 V and a 3 dB bandwidth of ∼100 GHz [29]. The dispersion in LN microring resonators [30] can be considered negligible for the relatively long input pulses that will be appropriately matched to the cavity roundtrip time. If we consider a cavity of net length 1.5 cm, out of which 0.5 cm accounts for the phase shifter region, the roundtrip time of the cavity is around 110 ps. A 100 GHz modulation rate corresponds to a rise time of a few picoseconds, which can be considered as rapid switching when compared to the roundtrip time of 110 ps. For an input pulse profile as shown in the inset of Fig. 2(d) of width 110 ps, taking the losses discussed above into account (∼0.13 dB per roundtrip while assuming an ideal splitter), it is possible to achieve a spectral compression factor of 92 (output spectral width of ∼100 MHz) and a peak power spectral density enhancement of ∼33 with a net loss of around 2.5 dB when we maintain $r_2 = 0.98$. However, if we could reduce the losses in the phase shifter section, which accounts for a significant portion of total loss, to the level of the straight waveguide section, it would be possible to achieve a spectral compression factor of ∼208 (output spectral width of ∼44 MHz) and a peak power spectral density enhancement of ∼93 for a net loss of 1.7 dB when we maintain $r_2 = 0.99$. The net loss can be reduced to ∼0.25 dB, but at a reduced spectral compression factor of ∼36 (output spectral width of ∼256 MHz) and a peak power spectral density enhancement of ∼22, when operated at $r_2 = 0.92$.

In summary, we have proposed a new electro-optic approach for spectral compression using time-varying cavities and discussed key design constraints. Since the system is linear, this spectral compression is equally applicable to classical light and light at the single photon level. It should also be possible to modify the temporal profile of the output pulse by dynamically tuning the reflectivity of the output mirror and to achieve spectral tuning and compression simultaneously via dynamic tuning of the refractive index. One may also use a nonlinear or time lens based spectral compression approach as a front end to our time-varying approach to achieve even larger spectral compression factors. Finally, one can envisage operating a time-varying cavity in the reverse sense, i.e., rapidly switching the output reflectivity from one to zero to achieve spectral broadening of a narrowband input after it is captured resonantly into the cavity.

Funding. National Science Foundation (ECCS-1809784); Air Force Office of Scientific Research (FA9550-15-1-0211).

Acknowledgment. The authors thank Hsuan-Hao Lu for insightful discussions.

Disclosures. The authors declare no conflicts of interest.

REFERENCES

1. M. Notomi and S. Mitsugi, Phys. Rev. A **73**, 051803 (2006).
2. S. F. Preble, Q. Xu, and M. Lipson, Nat. Photonics **1**, 293 (2007).
3. H. Lira, Z. Yu, S. Fan, and M. Lipson, Phys. Rev. Lett. **109**, 033901 (2012).
4. M. Zhang, B. Buscaino, C. Wang, A. Shams-Ansari, C. Reimer, R. Zhu, J. M. Kahn, and M. Lončar, Nature **568**, 373 (2019).
5. M. Kourogi, K. Nakagawa, and M. Ohtsu, IEEE J. Quantum Electron. **29**, 2693 (1993).
6. Z. Jiang, D. E. Leaird, C.-B. Huang, H. Miao, M. Kourogi, K. Imai, and A. M. Weiner, IEEE J. Quantum Electron. **43**, 1163 (2007).
7. M. Zhang, C. Wang, Y. Hu, A. Shams-Ansari, T. Ren, S. Fan, and M. Lončar, Nat. Photonics **13**, 36 (2019).
8. H. Gevorgyan, A. Khilo, and M. A. Popović, "Active-cavity photonic molecule optical data wavelength converter for silicon photonics platforms," arXiv preprint arXiv:2005.04989 (2020).
9. M. F. Yanik and S. Fan, Stud. Appl. Math. **115**, 233 (2005).
10. M. Heuck, K. Jacobs, and D. R. Englund, Phys. Rev. Lett. **124**, 160501 (2020).
11. H. J. Kimble, Nature **453**, 1023 (2008).
12. N. Nishizawa and K. Takahashi, Opt. Lett. **36**, 3780 (2011).
13. E. S. Lamb and F. W. Wise, Biomed. Opt. Express **6**, 3248 (2015).
14. H.-P. Chuang and C.-B. Huang, Opt. Lett. **36**, 2848 (2011).
15. J. Lavoie, J. M. Donohue, L. G. Wright, A. Fedrizzi, and K. J. Resch, Nat. Photonics **7**, 363 (2013).
16. A. Weiner, A. Kan'an, and D. Leaird, Opt. Lett. **23**, 1441 (1998).
17. Z. Zheng and A. Weiner, Opt. Lett. **25**, 984 (2000).
18. M. Allgaier, V. Ansari, L. Sansoni, C. Eigner, V. Quiring, R. Ricken, G. Harder, B. Brecht, and C. Silberhorn, Nat. Commun. **8**, 1 (2017).
19. M. Karpiński, M. Jachura, L. J. Wright, and B. J. Smith, Nat. Photonics **11**, 53 (2017).
20. F. Sośnicki and M. Karpiński, Opt. Express **26**, 31307 (2018).
21. F. Sosnicki, M. Mikolajczyk, A. Golestani, A. Widomski, and M. Karpiński, *CLEO: QELS_Fundamental Science* (Optical Society of America, 2020), paper FM1C-1.
22. M. Shirasaki, Opt. Lett. **21**, 366 (1996).
23. S. Xiao, A. M. Weiner, and C. Lin, IEEE J. Quantum Electron. **40**, 420 (2004).
24. A. M. Weiner, Appl. Opt. **51**, 8187 (2012).
25. A. Weiner, *Ultrafast Optics* (Wiley, 2011), Vol. **72**.
26. B. Crosignani, A. Yariv, and P. Di Porto, Opt. Lett. **11**, 251 (1986).
27. W. D. Sacher and J. K. Poon, Opt. Express **16**, 15741 (2008).
28. M. Zhang, C. Wang, R. Cheng, A. Shams-Ansari, and M. Lončar, Optica **4**, 1536 (2017).
29. C. Wang, M. Zhang, X. Chen, M. Bertrand, A. Shams-Ansari, S. Chandrasekhar, P. Winzer, and M. Lončar, Nature **562**, 101 (2018).
30. Y. He, H. Liang, R. Luo, M. Li, and Q. Lin, Opt. Express **26**, 16315 (2018).